Vietnam Journal
of MECHANICS

Volume 36 Number 2

$$\frac{2}{2014}$$

EXPERIMENTS AND NUMERICAL CALCULATION TO DETERMINE AERODYNAMIC CHARACTERISTICS OF FLOWS AROUND 3D WINGS

Nguyen Hong Son[1]**, Hoang Thi Bich Ngoc**[2,*]**, Dinh Van Phong**[2]**,
Nguyen Manh Hung**[2]
[1]*Hanoi University of Industry, Vietnam*
[2]*Hanoi University of Science and Technology, Vietnam*
*E-mail: hoangthibichngoc@yahoo.com
Received October 21, 2013

Abstract. The report presents method and results of experiments in wind tunnel to determine aerodynamic characteristics of 3D wings by measuring pressure distribution on the wing surfaces. Simultaneously, a numerical method by using sources and doublets distributed on panel elements of wing surface also is carried out to calculate flows around 3D wings. This computational method allows solving inviscid problems for wings with thickness profile. The experimental and numerical results are compared to each other to verify the built program that permits to extend the range of applications with the variation of wing profiles, wing planforms, and incidence angles.

Keywords: Experiment, singularity method, 3D wing.

1. INTRODUCTION

Singularity method using the surface distribution of sources and doublets with constant strength on panel elements is programmed for calculating flows over rectangular wings and trapezoidal wings with small sweep angles at the leading and trailing edges. The method is applied to calculate aerodynamic characteristics of flows around 3D wings in considering the profile thickness with the variation of incidence angles. The singularity method is based on Laplace equation of velocity potential for incompressible and inviscid flow. In the assumption of subsonic flow, incidence angles being not too large and sweep angles of wing having moderate values, results calculated by singularity method and calculated by viscous method are almost no different [1].

In order to verify the built code, the experimental study measuring pressure distributions on 3D wing was carried out in a wind tunnel. Wind tunnel used in this work is an open return wind tunnel having the test section dimension (400 mm × 500 mm) (at the Hanoi University of Science and Technology). Flow velocities in the wind tunnel with $M \leq 0.1$ are created by an exhaust axial fan. The surrounding walls of test chamber are made of transparent mica glass for the observation. Static pressures on the wing surface are

measured by a digital manometer of high quality [tolerance: $\pm 0.15\%$ of full scale ± 1digit $= (\pm 3 \pm 1)$Pa]. Wings used in the experiment are rectangular having the profile Naca 0012 with the variation of incidence angles. To ensure the accuracy of measurement results, procedures of processing have been built for working the wing geometry, the perforation of holes in the wing, and the assembly of flexible tubes connecting the holes inside the wing with the digital manometer.

2. NUMERICAL METHOD

Fig. 1 presents the mesh on wing surface with quadrilateral panel elements. Sources of constant strength σ and doublets of constant strength μ are distributed on the panel elements. The velocity potential φ at an arbitrary point is the summation of the velocity potential at infinity φ_∞ and the velocity potential induced from singularities (sources and the doublets) φ_i

$$\varphi = \varphi_\infty + \varphi_i,\tag{1}$$

where φ_i are induced from the source φ_S and the doublet φ_D.
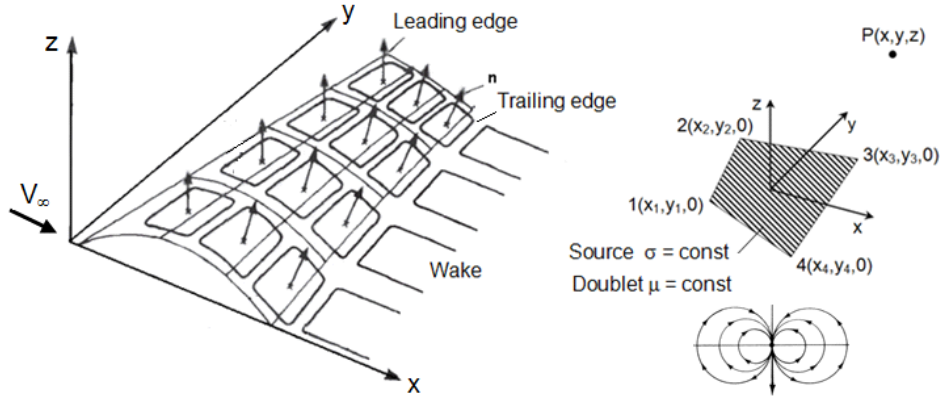

Fig. 1. Distribution of sources and doublets on panel elements of wing

Velocity potentials at a point $P(x, y, z)$ induced from sources of constant strength σ and doublets of constant strength μ are as follows [2, 3]

$$\varphi_S(x, y, z) = \frac{-\sigma}{4\pi} \int\limits_S \frac{dS}{\sqrt{(x - x_0)^2 + (y - y_0)^2 + z^2}},\tag{2}$$

$$\varphi_D(x, y, z) = \frac{-\mu}{4\pi} \int_S \frac{z\, dS}{\left[(x - x_0)^2 + (y - y_0)^2 + z^2\right]^{3/2}}.\tag{3}$$

The velocity components at a point are determined from the derivatives of velocity potential $(u, v, w) = (\varphi_x, \varphi_y, \varphi_z)$. About the boundary conditions, this problem uses Dirichlet condition for the internal potential $\varphi_{in} = (\varphi + \varphi_\infty)_{in} = const$

$$\boldsymbol{\sigma} = \mathbf{n} \cdot \mathbf{q}_\infty.\tag{4}$$

To satisfy Joukowski condition at the trailing edge, differences of doublet strengths on upper and lower panels are equal to doublet strengths of wake

$$(\mu_u - \mu_l) + \mu_w = 0 \,. \tag{5}$$

In the relations (4) and (5), $\mathbf{n}$ is the normal vector, $\mathbf{q}_\infty$ is the dynamic pressure, μ_u end μ_l are doublet strengths on upper and lower panels at the trailing edge, μ_w is the doublet strength of wake.
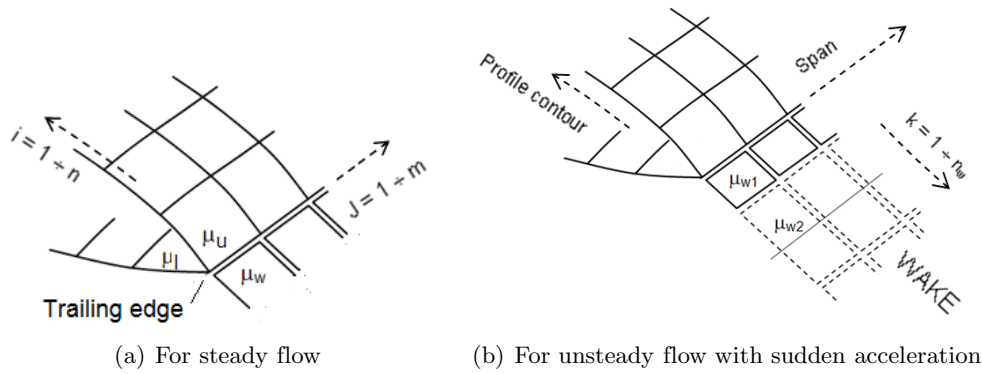

(a) For steady flow   (b) For unsteady flow with sudden acceleration

Fig. 2. Conditions at the trailing edge

For the steady flow, boundary conditions on the wing surface and Joukowski condition at the trailing edge indicate a system of $\{(n \times m) + m\}$ equations and $\{(n \times m) + m\}$ unknowns of doublet strength (n is the number of points discretized on the profile contour; m is the number of points discretized on the wingspan). For the unsteady flow with sudden acceleration, there are $\{(n \times m) + (n_w \times m)\}$ linear equations and $\{(n \times m) + (n_w \times m)\}$ unknowns (n_w is the number of steps for unsteady wake). On the algorithm of solving the system of linear equations for steady and unsteady problems, refer [4].

3. EXPERIMENTAL METHOD

3.1. Preparation for instruments and models of testing

The accuracy of measurement depends on the wind tunnel, experimental instruments and models for testing. As mentioned above, the wind tunnel and the Pitot tube made by Dantec Dynamics have high accuracy of measurement, and the digital manometer DM3501 made from Japan has a good quality. The measurement is also related to the accuracy of models on the shape of wing and the holes for measuring static pressures.

In order to ensure the smooth and avoid the deformation at the trailing edge and leading edge, wings are made from inox, and processed by CNC milling machine. The processing procedure for wings is fairly complicated when the gage holes are drilled in the wing, and the flexible air tubes connected from the holes to the digital manometer are completely arranged in the wing (see Fig. 3). Wings should be processed within the hollow and pressure gage holes are treated by CNC-EDM machine (electrical discharge machine).

Depending on the profile and the hole position, it is necessary to define the center axis of hole being perpendicular to the wing surface.
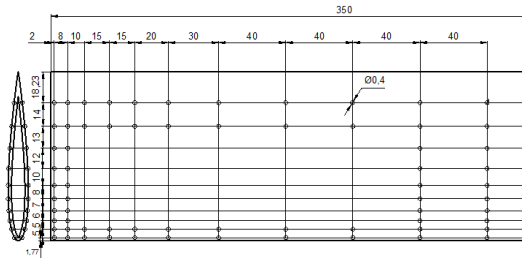

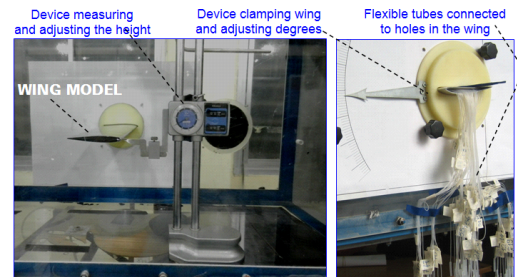*Fig. 3.* Scheme for perforation of holes in the wing for testing

Fig. 4. Fixing and adjusting wing models in the wind tunnel

Table 1. Parameters of wing models for testing

1	Rectangular wing with profiles	Naca 0012
2	Total wingspan	350 mm
3	Method of fixing wings	Clamped to the wall
4	Effective wingspan	< 260 mm
5	Chord	100 mm
6	Numbers of holes in the wing	20 holes $\times$ 11 row = 220 holes
7	Diameter of gage hole	0.4 mm

Parameters of wing models for testing are shown in the Tab. 1. The diameter of pressure gage hole is 0.4 mm, and there are 220 holes distributed more densely near the leading edge (along the movement direction) and near the wingtip (along the wingspan direction). For measuring aerodynamic characteristics of 3D wing, the wing is clamped to the wall of wind tunnel with the console mode that keeps a distance of (100÷140) mm between the wingtip and the wind tunnel wall. Therefore, it is necessary to make a solid jig for clamping the wing to wall so that the wing is able to carry itself weight and the aerodynamic load (Fig. 4).

3.2. Calibration

The calibration is required for all measurements. For these experiments, it is necessary to do calibration for experimental equipments and instruments.

3.2.1. *Calibration of initial values for experimental equipments*

It is required to do calibration for fixing the wing to ensure its axe being parallel to the bottom surface of test chamber, and then to calibrate zero value of incidence angle. The velocity uniform field of free flow in wind tunnel and its value is measured by a Pitot tube moving in the test chamber (Fig. 4 and Fig. 5).

3.2.2. *Calibration for the digital manometer*

Values of pressure difference captured from holes of wing can be identified by the digital manometer MD 3501, a converter and the Wave logger software as shown in Fig. 5.
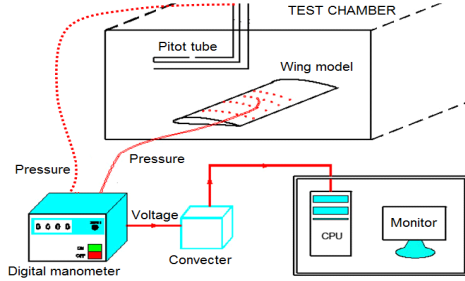

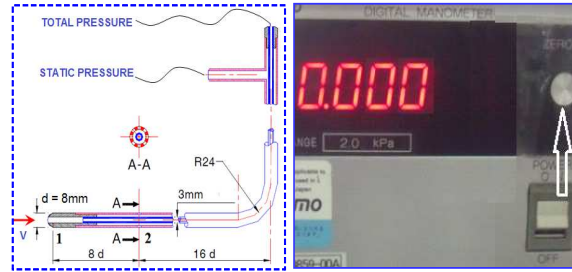*Fig. 5.* Equipment in the experimental system

Fig. 6. Pitot tube and adjusting zero value for the manometer

The calibration procedure for the digital manometer DM 3501 is executed step by step: turning it on, connecting to computer, installing the necessary data, adjusting zero value for the manometer. The zero point adjustment of DM 3501 is done by connecting two pressure plug holes of Pitot tube with two input plugs of manometer (see Fig. 5 and Fig. 6). When the wind tunnel is off, air flow velocity is zero, static and total pressures at two branches of Pitot tube are equilibrium $\Delta p = p_{static} - p_{total} = 0$, should then adjust zero point for the manometer. So in fact, the visualized measurement value is the difference between static pressure on wing surface and static pressure at infinity.

$$\Delta p_{\mathrm{mesure}} = p - p_{\infty} = \Delta p. \tag{6}$$

3.3. Treating and acquiring results

For taking the measurement value at a point, select 30000 measure times and average them. The time between two consecutive measurements is 1 ms. Pressure measured value $\Delta p_{\mathrm{mesure}}$ is an average of 30000 received values that is transferred to the computer for processing

$$\Delta p_{\mathrm{mesure}} = \sum_{i=1}^{30000} \Delta p_i. \tag{7}$$

The software processing measurement results installed on the computer allows displaying graphs of 30000 measuring times by electric voltage (mV) over time (Fig. 7), and exporting 30000 pressure values Δp_i and storing them in Excel tables (Fig. 7).

Pressure coefficient c_p is determined from the average of measured values $\Delta p_{\mathrm{mesure}}$

$$c_p = \frac{\Delta p_{\mathrm{mesure}}}{\frac{1}{2}\rho V_{\infty}^2}, \tag{8}$$

where ρ is the air density (temperature in the laboratory $T = 30°\mathrm{C}$, $\rho = 1.14\,\mathrm{kg/m^3}$); V_{∞} is the velocity of free flow in the wind tunnel.
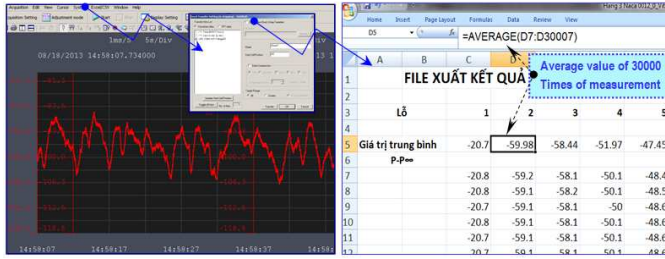
Fig. 7. Interface displaying graph of 30000 measuring times and command exporting them to Excel file
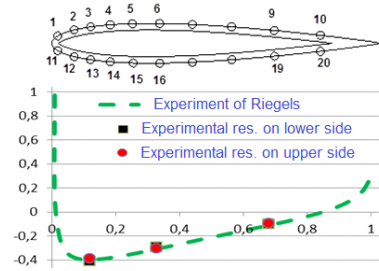

Fig. 8. C_p for symmetric case $\alpha = 0°$

Fig. 8 presents experimental results on pressure coefficient for test in a symmetric case ($\alpha = 0°$) at the hole row right near the wing root. It is observed that measurement results at two upper and lower sides are almost identical and similar to experimental result of Riegels [5]. That is a reliable base for conducting other measurements for 3D wings. After performing calibration, it is possible to measure pressures on upper and lower 3D wing surfaces. For one value incidence angle, it is necessary to measure pressures at 220 holes (Δp_{mesure}) on the wing surface. The analysis of experimental and numerical results is presented in the next part.

4. RESULTS OF EXPERIMENTS AND COMPUTATIONS

It is clear that the precision of measuring pressure distributions on the wing surface depends on the machining quality of surface and pressure gauge holes. Flexible tubes in the wing with small diameter (0.4 mm) can be pinched or crushed by turn directions. This requires very careful manipulation in the process of experiments.

Fig. 9 presents the 3D distribution of the pressure coefficients determined by the measurement results compared with the results calculated by the 3D code of singularity method using sources and doublets. As mentioned above, the experimental pressure at each point is the average of 30000 times of measurement. The implementation in the form of bi-dimensional graphs facilitates the observation and the comparison. It is shown that experimental results and numerical results are similar.

Experimental results for case of incidence angle $\alpha = 4°$ are presented in Fig. 10. On each bi-dimensional section there are 20 points measuring pressure, which are compared with numerical results calculated by the built 3D code. The comparison of results on bi-dimensional sections shows good agreement between the experimental results and the numerical results. The comparison of results in form of 3D graphs shows a view of the pressure coefficient distribution on the 3D wing.

For the incidence angle $\alpha = 8°$, there is not yet a strong flow separation on the wing, experimental results and computational results of pressure coefficients calculated from the built code are similar for all bi-dimensional graphs, that is observed in Fig. 11.

Especially, pressures measuring at the row of holes near at the wingtip for three cases of incidence angles $\alpha = 2°$, $\alpha = 4°$, $\alpha = 8°$ are strongly impacted by the effect of wingtip that will be analyzed and presented in detail in the next report. Likewise, for

measurement results with very large incidence angles, the phenomenon of flow separation is very important, and they should be analyzed in detail in other reports.
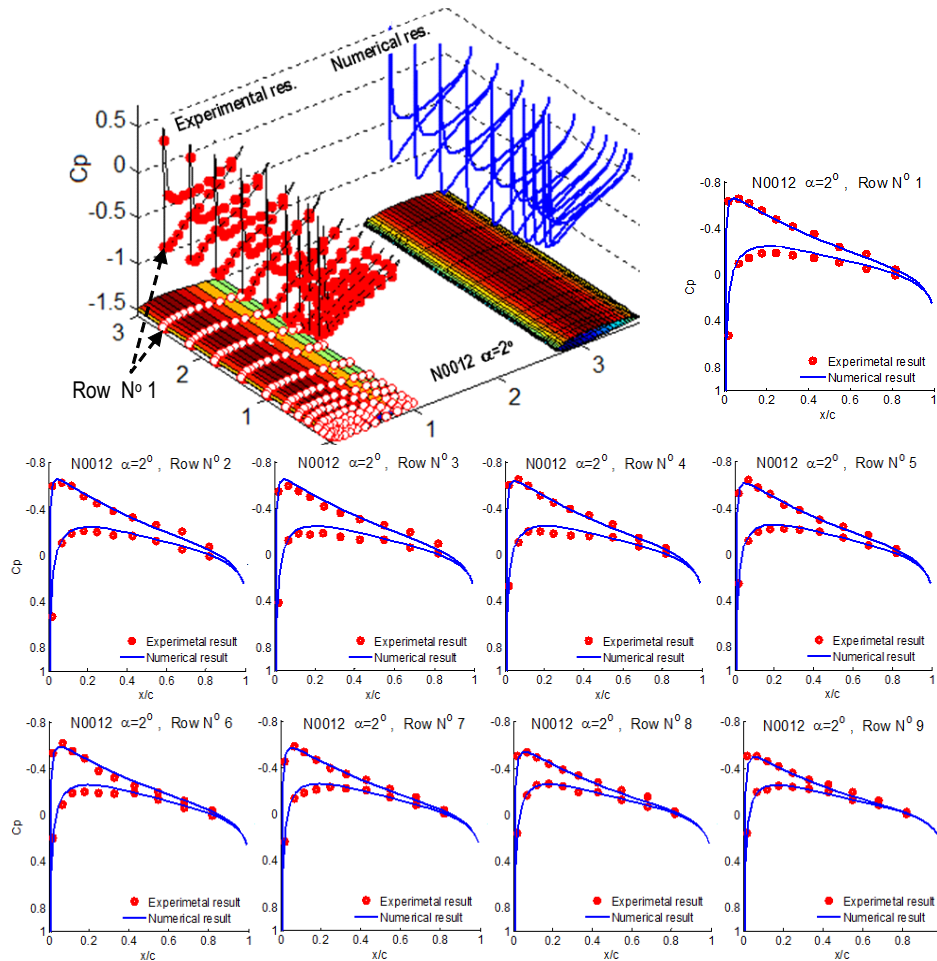

Fig. 9. Results of experiment and computation (by built 3D code)-3D pressure coefficients and implementation on 2D graphs ($\alpha = 4°$)

The experimental results determine the pressure distribution on 3D wing with high accuracy (as shown in Figs. 9-11) are very precious and essential in the study. However, the empirical research is so elaborate and costly in terms of effort and time. About the numerical method, once it is verified for accuracy of programming code, it would be more economical. Results in Fig. 12 are 3D distributions of pressure coefficients on cross-sections perpendicular to the wingspan (with the number of sections being many arbitrary), and results at $\alpha = 8°$ corresponding to two experiments are presented in Fig. 11.

Results of the lift coefficient distribution on wingspan corresponding to three experiments in Figs. 9-11 are also shown in Fig. 12. It observed that the lift coefficient of this 3D wing strongly increases with the incidence angle. The wing for test has the aspect

ratio $\lambda = 5.2$ ($c = 100$ mm), it is small for incompressible flows. In this case, the effect of wingtip strongly influences the lift coefficient. Compared with values of lift coefficient for the wing with infinite span (2D profile), values of lift coefficient for the finite wing of test (3D) here are smaller than about 30%.
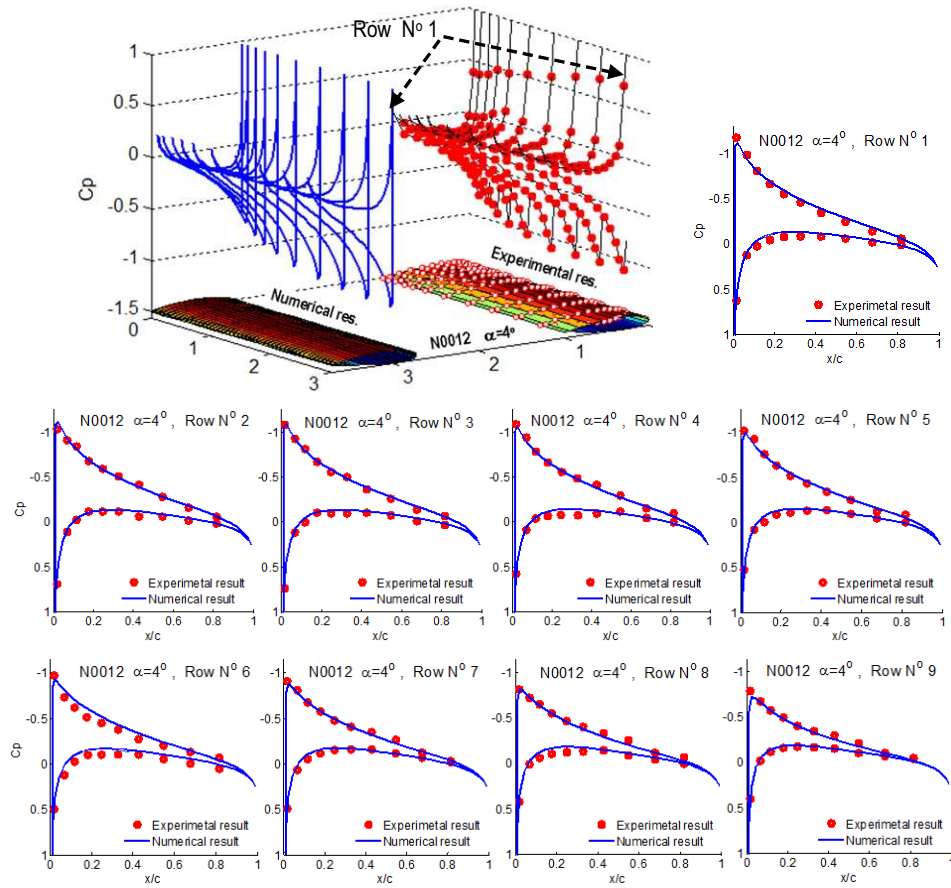

Fig. 10. Results of experiment and computation (by built 3D code)-3D pressure coefficients and implementation on 2D graphs ($\alpha = 2°$)

The consideration of the finite wingspan effect to lift coefficient is not difficult by using the built code. However, an important objective of this report is to present a methodology of measurement and experimental results for 3D wing, so the wing model for test is limited by the experimental laboratory equipment. The width of test section of wind tunnel is 400 mm only allows experiments with wings having the maximum aspect ratio $\lambda = 5.2$. If taking $\lambda > 5.2$, measurement results will be wrong due to the influence of the effect of wind tunnel walls. If the experiment is done for the 2D case in this wind tunnel, the aspect ratio is then $\lambda = 8$, that is considered as infinite wingspan (as 2D problem) and we have done with them in [6, 7], see also [8].
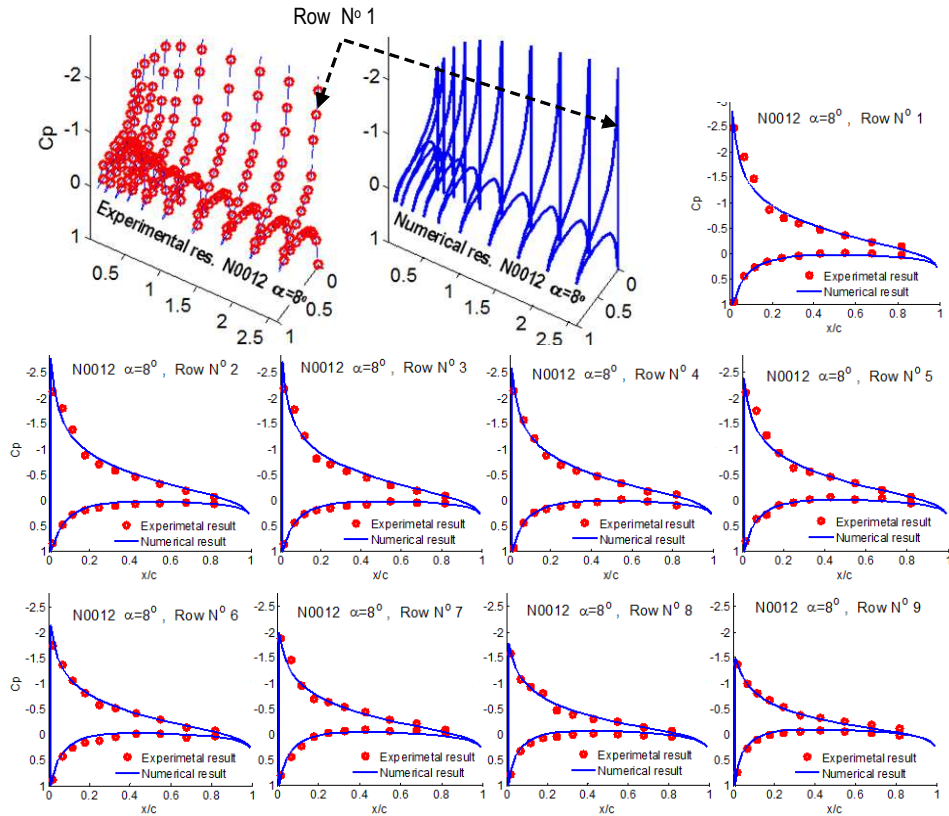
Fig. 11. Results of experiment and computation (by built 3D code)-3D pressure coefficients and implementation on 2D graphs ($\alpha = 8°$)
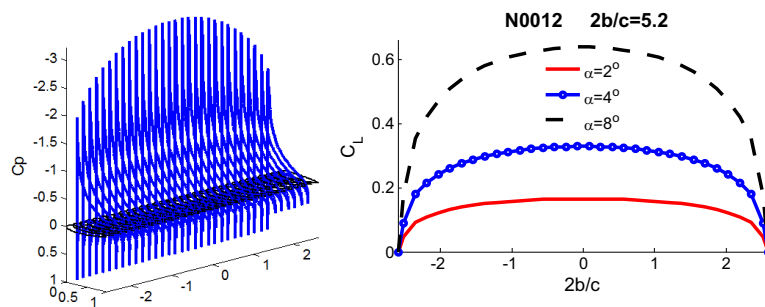

Fig. 12. 3D distribution of pressure coefficients ($\alpha = 8°$), and lift coefficient on wingspan ($\alpha = 2°$, $\alpha = 4°$, $\alpha = 8°$)

Fig. 13 presentes results on lift coefficient depending on incidence angles for the testing wing with the comparison of 3D present numerical result, 3D present experimental result (for 8 cases: $\alpha = 0°$, $2°$, $4°$, $6°$, $8°$, $10°$, $12°$, $14°$), 3D viscous Fluent result and 2D result [9]. This comparison shows the difference of results for the 3D case and the 2D
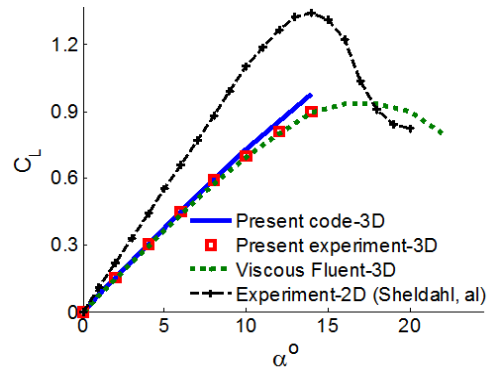
Fig. 13. Lift coefficient with incidence angles for testing wing-comparison
of 3D numerical and 3D experimental results (2D source [9])

case and the difference between inviscid and viscous results. For incidence angles $\alpha \leq 8°$, 3D experimental result and 3D viscous numerical result are similar to inviscid numerical result.

5. CONCLUSIONS

Singularity method with the distribution of sources and doublets on panel elements of wing surface is an effective method to calculate aerodynamic characteristics for 3D wings. This method allows calculating flows around 3D wing considering the effect of thickness profile. For subsonic flows, when the incidence angle is not too large so that there is not a strong separation of boundary layer, results on the distribution of pressure coefficients and lift coefficients calculated by inviscid flow method and viscous flow method are almost similar. Accordingly, the application of singularity methods is more economic than the methods of differential equations on amount of calculations, volume of computer memory and running time. Once a programmed code is verified about the accuracy, it can be extended for applications, so that may allow selection of optimal aerodynamic shapes for wings. By using the linear theory, this 3D built code can be applied to flows with free Mach numbers $M_\infty < 0.65$, to the extent that there is not any supersonic zone in the agitated domain. It means that the code is applied to compressible flows but not applicable to transonic flows.

It can be said that experimental studies are needed and should be combined with numerical methods, especially for 3D problems. In this study, experimental method is to determine static pressures on the wing surface, from that the lift coefficient is determined. This experimental method is different from the method of measuring the lift by using aerodynamic balance (each measurement can get a lift value). Meanwhile for the present experiment, in order to obtain a lift value, it is necessary to perform 220 measurements for 220 pressure gage holes in the wing.

The experimental method measuring pressures on 3D wing allows determining the distribution of aerodynamic load on the wing (differences of pressures on upper and lower

wing surface) that is related to the calculation of wing structures. And aero-elasticity problem is a part of our related research, which will be presented in the next report.

However, the measurement of the pressure distribution on the wing is attached to certain difficulties and complexities for preparing test models and experimental equipments. In addition to the required high accuracy of measuring instruments, pressure gage holes in the wing should be small enough and they need to be assured perpendicular to the wing surface. All the flexible air tubes connected from the holes to the digital manometer are completely arranged in the wing in order to avoid disturbing the flow. It is required a careful technological processes to manufacture a wing within the hollow having 220 pressure gage holes of diameter 0.4 mm in the wing.

The similarity between the measurement results and the numerical results allows expanding applications of the built code, and likewise, this experimental methodology enables to be applied to further studies for slow speed aircraft.

REFERENCES

[1] H. T. Bich Ngoc and N. M. Hung. Study of separation phenomenon in transonic flows produced by interaction between shock wave and boundary layer. *Vietnam Journal of Mechanics*, **33**, (3), (2011), pp. 170–181.

[2] H. Schlichting, E. Truckenbrodt, and H. J. Ramm. *Aerodynamics of the Airplane*. McGraw-Hill New York, (1979).

[3] J. Katz and A. Plotkin. *Low-speed aerodynamics*. McGraw-Hill, USA, (1991).

[4] N. M. Hung, H. T. Bich Ngoc, and N. H. Son. Calculating aerodynamic characteristics of swept-back wings. In *Proceedings of The 14th Asia Congress of Fluid Mechanics*, Hanoi, (2013). pp. 132–137.

[5] F. W. Riegels. *Aerofoil sections*. Butterworths Pub., London, (1991).

[6] H. T. Bich Ngoc, N. M. Hung, and N. T. Mich. Velocity measurements on profile by means of laser measurer. In *Proceedings of national Conference on Metrology*, (2010), pp. 438–448.

[7] N. M. Hung and H. T. Bich Ngoc. Experimental study of laminar separation phenomenon combining with numerical calculations. *Vietnam Journal of Mechanics*, **33**, (2), (2011), pp. 95–104.

[8] I. Balaguru and S. Sendhilkumar. Numerical and experimental investigation on aerodynamic characteristics of sma actuated smart wing model. *International Journal of Engineering & Technology*, **5**, (5), (2013), pp. 3813–3818.

[9] R. E. Sheldahl and P. C. Klimas. Aerodynamic characteristics of seven airfoil sections through 180 degrees angle of attack for use in aerodynamic analysis of vawt. Energy report, Sandia national laboratories-USA, (1981).

CONTENTS

Pages